The Astrophysical Journal, 694:1664–1669, 2009 April 1 doi:10.1088/0004-637X/694/2/1664

AMiBA: BROADBAND HETERODYNE COSMIC MICROWAVE BACKGROUND INTERFEROMETRY

Ming-Tang Chen[1], Chao-Te Li[1], Yuh-Jing Hwang[1], Homin Jiang[1], Pablo Altamirano[1], Chia-Hao Chang[1], Shu-Hao Chang[1], Su-Wei Chang[1], Tzi-Dar Chiueh[2], Tah-Hsiung Chu[2], Chih-Chiang Han[1], Yau-De Huang[1], Michael Kesteven[3], Derek Kubo[1], Pierre Martin-Cocher[1], Peter Oshiro[1], Philippe Raffin[1], Tashun Wei[1], Huei Wang[2], Warwick Wilson[3], Paul T. P. Ho[1,4], Chih-Wei Huang[2], Patrick Koch[1], Yu-Wei Liao[2], Kai-Yang Lin[1,2], Guo-Chin Liu[1], Sandor M. Molnar[1], Hiroaki Nishioka[1], Keiichi Umetsu[1], Fu-Cheng Wang[2], and Jiun-Huei Proty Wu[2]
[1] Academia Sinica, Institute of Astronomy and Astrophysics, P.O. Box 23-141, Taipei 106, Taiwan; mchen@asiaa.sinica.edu.tw
[2] National Taiwan University, Taipei 106, Taiwan
[3] Australia Telescope National Facility, P.O. Box 76, Epping, NSW 1710, Australia
[4] Harvard-Smithsonian Center for Astrophysics, 60 Garden Street, Cambridge, MA 02138, USA
Received 2008 December 9; accepted 2009 February 6; published 2009 March 25

ABSTRACT

The Y. T. Lee Array for Microwave Background (AMiBA) has reported the first results on the detection of galaxy clusters via the Sunyaev–Zel'dovich effect. The objectives required small reflectors in order to sample large-scale structures (20′), while interferometry provided modest resolutions (2′). With these constraints, we designed for the best sensitivity by utilizing the maximum possible continuum bandwidth matched to the atmospheric window at 86–102 GHz, with dual polarizations. A novel wide-band analog correlator was designed that is easily expandable for more interferometer elements. Monolithic millimeter-wave integrated circuit technology was used throughout as much as possible in order to miniaturize the components and to enhance mass production. These designs will find application in other upcoming astronomy projects. AMiBA is now in operation since 2006, and we are in the process to expand the array from seven to 13 elements.

Key words: cosmic microwave background – cosmology: observations – instrumentation: interferometers

Online-only material: color figures

1. INTRODUCTION

Array for Microwave Background (AMiBA; Lo et al. 2002; Ho et al. 2009) is a sensitive interferometer operating at 3 mm wavelength to study the spatial structure of the cosmic microwave background (CMB). The goal is to complement the existing and planned projects in cosmology, such as the Degree Angular Scale Interferometer (DASI; Halverson et al. 2002), the Cosmic Background Imager (CBI; Padin et al. 2002), and the *Wilkinson Microwave Anisotropy Probe* (*WMAP*; Bennett et al. 2003). In particular, AMiBA is imaging clusters via the Sunyaev–Zel'dovich effect (SZE; Sunyaev & Zel'dovich 1970, 1972) for the first time at 3 mm wavelength. Our instrumentation is realized due to the maturity of low-noise, wide-bandwidth microwave components in the *W* band (75–110 GHz), as demonstrated by Erickson et al. (1999) and Pospieszalski et al. (2000). The choice of instrument has been fostered by our technical expertise and interest that grew out of the previous collaboration on the Submillimeter Array project (Ho et al. 2004).

Radio interferometry is inherently a signal-differencing instrument. It has the advantage in stability and the inherent spatial filtering function, which are suitable for observing CMB and SZ targets with very low systematic error. It has the capability to reject common mode noise usually present in a multielement array detector system, and to reach intrinsically fainter sensitivities. These technical characteristics attract a number of cosmology projects utilizing interferometry technique (Carlstrom et al. 2002). AMiBA follows the lead of these earlier projects but we exploit the 3 mm band.

The performance of heterodyne receivers in noise temperature is already near its theoretical limit at 3 mm. To further improve sensitivity, we have to increase the number of the antennas and/or broaden the instantaneous bandwidth of observation. Thus, we opted to build a scalable system with as broad a bandwidth as possible. We had specified an intermediate frequency (IF) of 2–18 GHz based on commercial availability. A larger bandwidth would have been much more expensive in construction cost. We matched this IF window to the atmospheric window at 86–102 GHz.

The AMiBA scientific goals and design philosophy are presented in Ho et al. (2009). The telescope and its operational performance are described in Koch et al. (2009). Lin et al. (2009) gives further details on the observational performance of AMiBA. The early results, carried out with the 7 m × 0.6 m antennas, have been reported in a series of companion papers (Nishioka et al. 2009; Wu et al. 2009; Umetsu et al. 2009). The array was dedicated with its compact seven-element configuration in 2006, and the instrument has been constantly operating ever since. We are now replacing the reflectors with their 1.2 m counterparts. We are also expanding the array from 7 to 13 elements. The following section gives an overview on the components of the AMiBA instrumentation.

2. INSTRUMENTATION

We designed, tested, and prototyped our components to optimize broadband sensitivity (Chen et al. 2002; Li et al. 2004). The current instrument specifications are listed in Table 1, and Figure 1 shows the block diagram of the overall system. We describe below the various features which optimized AMiBA sensitivity, and which can be further enhanced in the future for other applications.

Receiver optics. The receiver optics is composed of a Cassegrain reflector coupled to a corrugated scalar feed. The feed has a semiflare angle of 14° to ensure an approximate constant beam

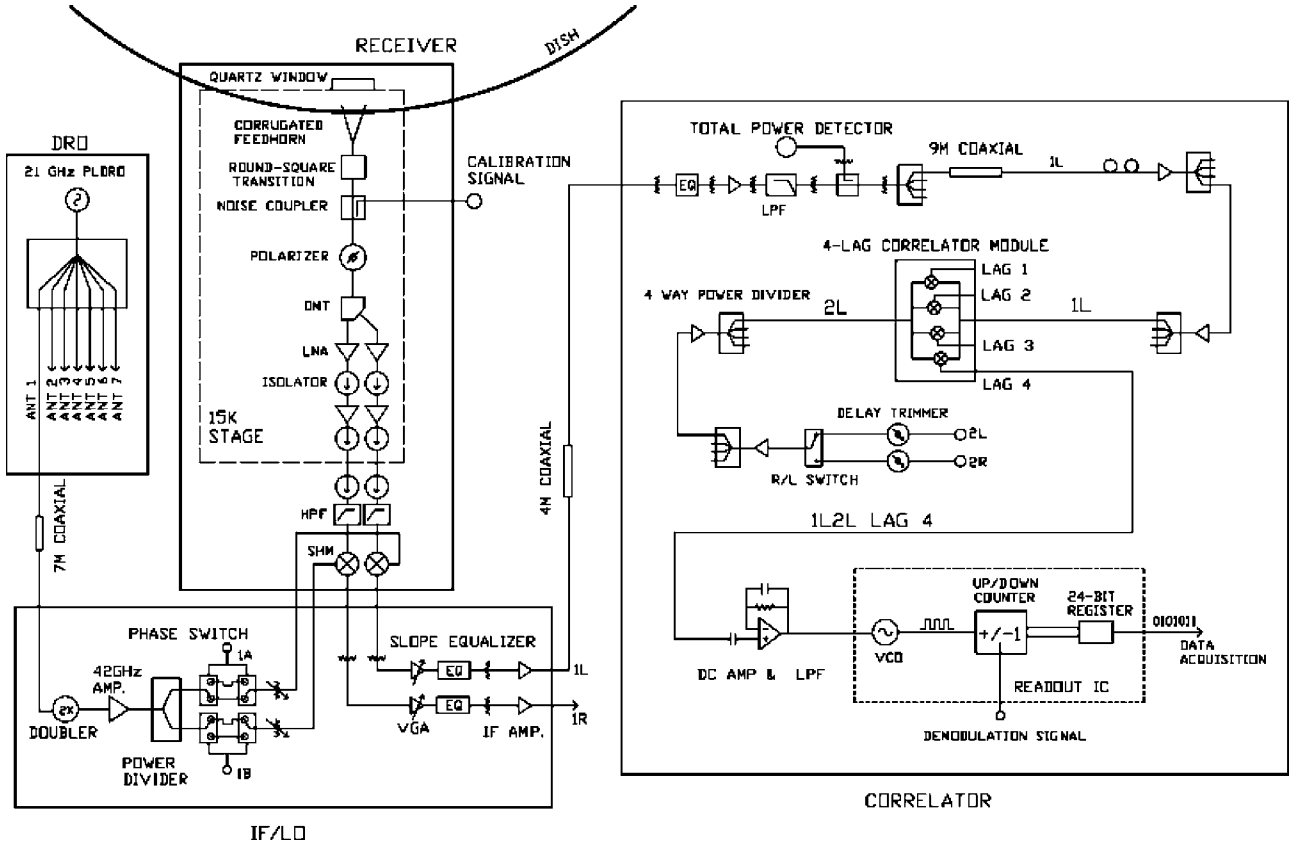

Figure 1. System block diagram for the AMiBA receiver and correlator configuration.

Table 1
AMiBA Detection System Characteristics

Components	Specifications
Cassegrain reflector, f/2.0	0.6 m and 1.2 m Interchangeable
Receiver front-end	MMIC HEMT LNA
	Dual polarization
	Cooled to 15 K
RF	86–102 GHz
Receiver noise temperature	65 ± 10 K
Down-conversion	Subharmonic mixer
LO frequency	42 GHz with phase-switching
LO source	Dielectric Resonator Oscillator at 21 GHz
IF	2–18 GHz
	Variable gain control
Correlator	Analog correlation
	Four lags
	Diode multiplier

width over the receiver band (Padin et al. 2002; Clarricoats & Olver 1984). Based on a quasi-optics method described in Goldsmith (1998), the feed is designed to illuminate the reflector with an edge taper of 10.5 dB. The beam waist produced from this feed is located at the vertex of the Cassegrain dish. The advantage for such arrangement is that we can outfit the receiver with reflectors of different apertures. For the physical layout, this feed-horn is similar in design to those used in the Submillimeter Array receivers (Zhang 1993) for achieving a wide-band single mode operation, and a wide-band, low return loss simultaneously.

The antenna is a small-size Cassegrain reflector made of Carbon-Fiber-Reinforced Plastic (CFRP). We have two sizes of reflectors, 0.6 m and 1.2 m, for different scientific targets. Having several antennae in a close-packed configuration on the platform can cause cross-talk problems. Thus, our reflectors have baffles attached with a height of about 30% of the diameter in order to suppress cross talk and ground pickup. The edges of the baffles are slightly rolled in order to suppress diffraction effects. The design and fabrication of these reflectors in Taiwan established a team which has gone on to produce nutating subreflectors for the Altacama Large Millimeter/Submillimeter Array (ALMA) project under construction in Chile.

The reflector's surface is coated with aluminum. Aiming at minimizing a possible emission from the underlying material and maximizing the reflection of the incoming signal, an aluminum layer attenuation of less than 1% is targeted. A five times skin depth leads to an $e^{-5} = 0.67\%$ attenuation, which translates into about a 1.4 μm coating layer at the relevant frequency. By asking for at least 2.8 μm coating we are ensuring a very low attenuation.

After assembling, the geometry of the primary and the secondary reflectors is verified directly on a Zeiss Prismo 10 metrology machine. For the sizes of the AMiBA reflector, the measuring accuracy is better than 5 μm. We have specified a surface accuracy of 50 μm rms to ensure a gain efficiency of at least 95%. The subreflector positioning requirements are based on the Ruze formulae (Ruze 1966). An axial and lateral secondary defocus of 0.1 λ and 0.45 λ, respectively, keep the gain loss at less than 1%. ($\approx$3 mm at 90 GHz.) Similarly, a feed horn positioning within 1 λ gives a 99% gain.

Dual polarization front-end. The receiver front-end contains the scalar feed followed by a noise coupler, a phase shifter, and an orthomode transducer (OMT) for polarization separation (Wollack et al. 2002). A short section of 90° phase shifter

is connected to the OMT to perform a linear-to-circular polarization transformation. Currently this phase shifter is replaced with a simple waveguide transition, thus we are observing in linear polarization detections. These OMTs show typical insertion losses of less than 0.2 dB, return loss around 20 dB, and more than 40 dB isolation over the 75–110 GHz band. Similar OMTs have been used in the *WMAP* and ALMA (Claude et al. 2005). The availability of dual polarizations increases our sensitivity by a factor of $\sqrt{2}$, and will enable studies of polarization in the future.

After the OMT, each polarized signal then passes through its own chain of amplifiers, isolators, and a high-pass filter before reaching a subharmonic mixer. Two cascade amplifier modules and two wide-band WR-10 cryogenic isolators form the radio frequency (RF) amplifier chain. Each amplifier module contains a four-stage, InP high electron mobility transistor (HEMT), which is fabricated as a monolithic millimeter-wave integrated circuit (MMIC; Weinreb et al. 1999). Measured at 20 K cryogenic temperature, its noise temperature is typically 40–50 K, with associated gain higher than 22 dB over 80–105 GHz. The same low-noise amplifier (LNA) chip has been used in several other astronomical experiments; e.g., the Cosmic Anisotropy Polarization Mapper (CAPMAP) of Princeton University, the Sunyaev–Zel'dovich Array (SZA) of the University of Chicago, and the Second Quabbin Optical Imaging Array (SEQUOIA) from the University of Massachusetts (Erickson et al. 1999).

The filter before the mixer is designed with the cutoff frequency at 84.5 GHz (Liu et al. 2003). It enables an upper sideband conversion for the following mixer. Developed in-house (Hwang et al. 2002a, 2002b), a subharmonically pumped (SHP) diode mixer module mixes the 86–102 GHz RF signal with the 42 GHz local oscillator (LO) and generates an IF of 2–18 GHz. This mixer has achieved a flat response in the conversion loss of around 12 dB at an optimal LO power level of 7 dBm. The development of MMIC technology in Taiwan enhances the potential to mass produce large format array detectors. This can drive the future of multipixel heterodyne interferometry. The HEMT technology is also being developed for ALMA Band 1 receivers.

While the entire front end is enclosed in a vacuum chamber, only the components prior to the high-pass filter are cooled by the CTI-22 coldhead. This is to minimize the thermal loading on the coldhead, and to achieve a relatively simple mechanical design for the cryogenic environment. We used a z-cut quartz with antireflection coating as the vacuum window.[5] This coated quartz window comes in with 3 mm thickness and 35 mm in diameter. Its power transmission in the band of our interest has been measured using a vector network analyzer. With a time-gating technique (Ediss et al. 2000), the signal transmission is measured to be better than 97% in 80–105 GHz.

After down-conversion by the SHP, the IF signals are sent out of the cryostat and fed into the IF/LO module for further signal amplification. LO-phase switching is accomplished by using a pair of PIN switches and delay lines. This created an unexpected power variation for mixer LO drive. Although small, the subsequent IF levels become imbalanced and produce a systematic DC offset from the correlator output. The LO is intentionally adjusted to overpump the mixer to reduce this effect. The development of broadband LNA and SHP are key to reducing component costs, miniaturization, and lowering the weight of the receiver packages. Figure 2 shows the AMiBA front end with the vacuum jacket removed.

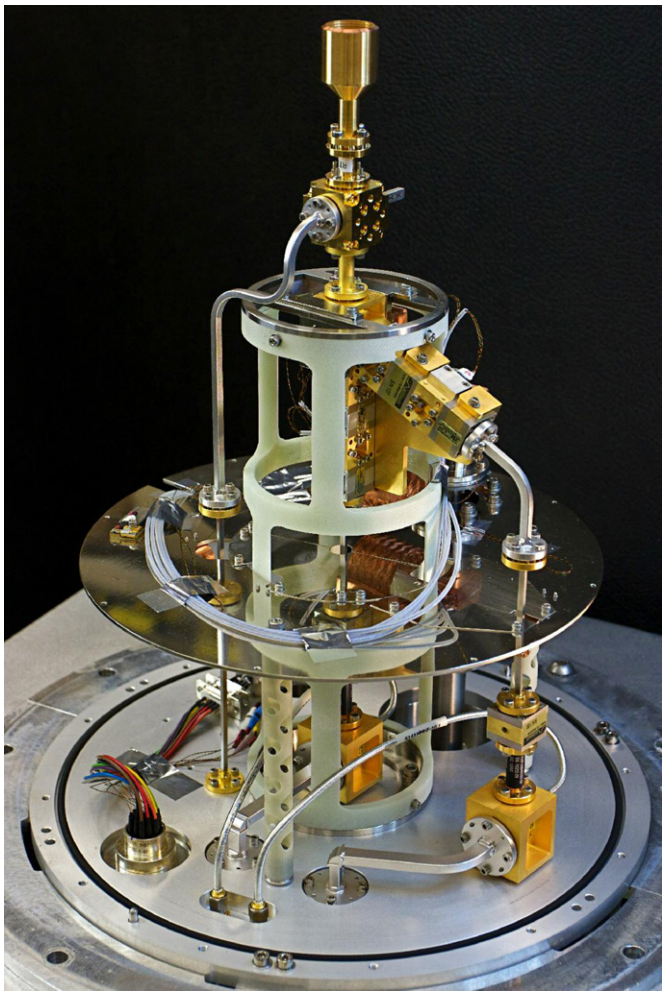

Figure 2. AMiBA receiver with vacuum jacket removed.

Signal distribution and correlation. The instantaneous bandwidth of 16 GHz in IF presents a major technical difficulty for the signal processing after the receiver front end. It is a great technical challenge to effectively distribute these multioctave signals through an interconnected network. Physically, each of the IF signal paths is designed with two four-way power dividers in cascade and a total of 13 m, semirigid coaxial cable between the SHP mixer and the correlator. To compensate for the signal transmission loss and the incurred bandwidth slope, the signal distribution network encompasses a series of power amplifications, power dividing, filtering, and slope correction. Active temperature compensation mechanisms are built into all the enclosed electronic modules. In all, although there is more than 150 dB active power gain in a single path, the IF network only provides a net gain of 36 dB, with a noise figure of about 10 dB between the SHP mixer and the correlator

Following on the development in broadband, lag-correlator by Harris & Zmuidzinas (2001), we designed and built a four-lag, analog correlator to achieve the unprecedented correlation bandwidth. The correlator module with four different delays yields complex visibility data in two bands. Each lag spacing is 25 picoseconds to sample signals up to 20 GHz of bandwidth. The decision on the number of the lags was another compromise between the cost and the performance. A doubly balanced diode

[5] The windows are manufactured by QMC Instrument Ltd.

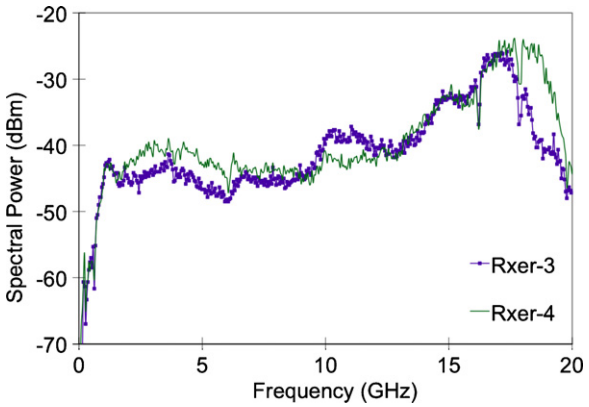

Figure 3. IF power spectra of the AMiBA receivers No. 3 and No. 4. (A color version of this figure is available in the online journal.)

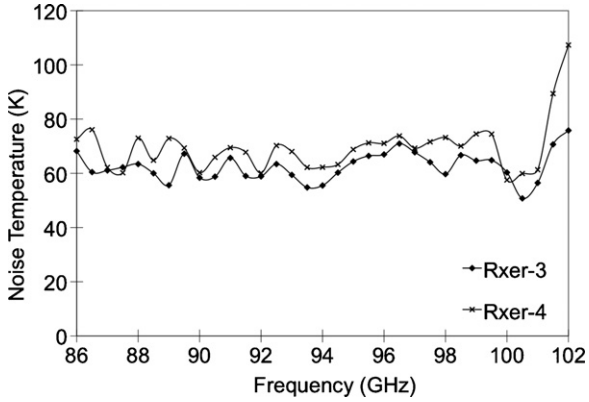

Figure 4. Receiver noise temperatures over the AMiBA RF band on two selected receivers, No. 3 and No. 4. The markers represent the data points.

mixer is chosen as the correlation multipliers to cope with broadband correlation. The passive multipliers avoid problems of $1/f$ noise, and the circuitry complications associated with active multipliers. The issue of high input impedance associated with nonbiased mixer is mitigated with the low barrier diodes chosen for the multiplier design. The diode mixers are usually broadband devices. It is the matching circuitry between the diodes and the input IF signals that dominates the effective bandwidth of the AMiBA correlator.

The correlated outputs are amplified and then digitized by custom-designed readout integrated circuits (ICs). Inside the readout IC, voltage-control oscillators (VCOs) implement the voltage to frequency conversion at 8 MHz, and the following up/down counters integrate the clock signal for a short period of time. Each of the IF signal is phased–switched at the down-conversion following an exclusive set of Walsh time sequences. After the signal correlation, the demodulation signal is applied to the up/down counter. The combination of the phase switching and the demodulation process can reject any false signals that do not have the corresponding signature as the demodulation signal.

3. SYSTEM PERFORMANCE

The receiver passband typically has considerable larger gain toward high frequency. This is mainly from the gain profile of the first slope equalizers in the IF chain, and it actually compensates for the gain slope caused by the long cables in the distribution network. Figure 3 shows the output spectra on some selected AMiBA receivers. The receiver noise temperature is measured using a conventional Y-factor method at room temperature with liquid-nitrogen-bath absorber as a cold load. Measured after the first IF amplifier, all the receivers show consistent noise performance with values ranging in 55–75 K, and with slight degradation near the high end of the band. Figure 4 plots the noise temperatures over the RF band on two of the selected AMiBA receivers. The LNA typically contributes about 50 K in the overall receiver noise temperature. The rest of the noise contribution is from the passive waveguide losses in front of the first LNA. This nontrivial noise contribution is a compromise from our intention for calibration and for detecting circular polarizations.

The inputs to the AMiBA correlators are dominantly the uncorrelated noises from the front ends amplified by the system gain before the correlators. The internal noise of the AMiBA correlators is small compared with these inputs and can be ignored in the system performance consideration. The cross-correlation of these noises in each baseline produces the low-frequency fluctuations at the correlator outputs and limits the correlator sensitivity. On the other hand, when there is a common signal present in the baseline, the correlator produces a correlated signal at 700 Hz, which is the phase modulation rate. The ratio of the root-mean-squared amplitudes of this 700 Hz signal over the low-frequency fluctuations is defined as the signal-to-noise ratio (S/N) for our detection system. Our effort is to tune the system to achieve the best S/N with reliable performance.

A group of randomly selected correlator modules are tested in the laboratory to determine the optimal input powers to the correlator for the best output S/N. The test is to measure the correlator's output S/N versus input power applied to the correlator. To simulate the observation, the input for the test consisted of a large uncorrelated noise mixed with a small common signal. The input S/N is kept at a nominal value of -20 dB throughout the test. All the correlators tested show very similar characteristics. One set of the test results are depicted in Figure 5. Within the tested power range, the output S/N has a relatively steep minimum around 0.2 mW, and then increases and approaches a saturated value at the high input beyond 2 mW. The increase in the output S/N at high driving power is mostly due to the increase in the output signal level, while the rms level of the low-frequency fluctuations stays almost the same beyond 0.5 mW. We have concluded that the AMiBA correlator modules deliver better output S/N with high level of uncorrelated driving power. In a following test, we measured the signal output linearity particularly at high driving power. As depicted in Figure 6, the output signal level remains in very good linearity with the balanced input signal, while the correlator is driven by high noise power at 1 mW. These results suggest that we should set up a high-gain power system before the correlators.

In reality, it is very difficult to maintain balanced inputs to the correlators, especially in a wide-band system (Padin 1994). One must consider the imbalance of the IF power levels due to the LO switching and the different gains of the signal path. More seriously, there is the passband mismatch between the IF signals (Thompson & D'Addario 1982). We have measured the correlator's output S/N versus the imbalanced input power levels. In these measurements, the input S/N is still fixed at -20 dB, while the pair of inputs to the correlator differ in power by 3 dB, or by a factor of 2, with the power ranging from -6 dBm to 3 dBm. The output S/N from these measurements

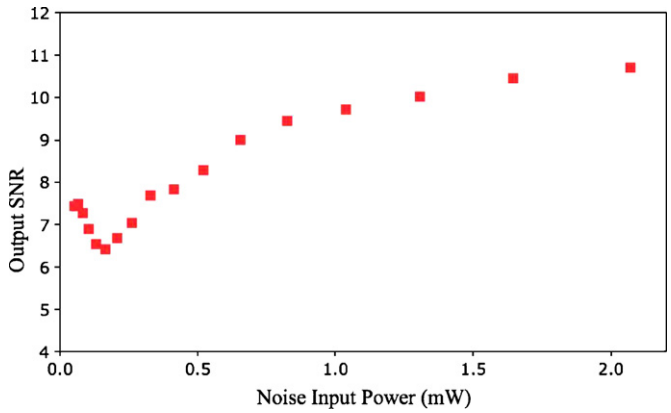

Figure 5. Typical output S/N of the AMiBA correlator vs. balanced input power. This measurement is for determining the nominal input power level to endure an optimal correlator operation.

(A color version of this figure is available in the online journal.)

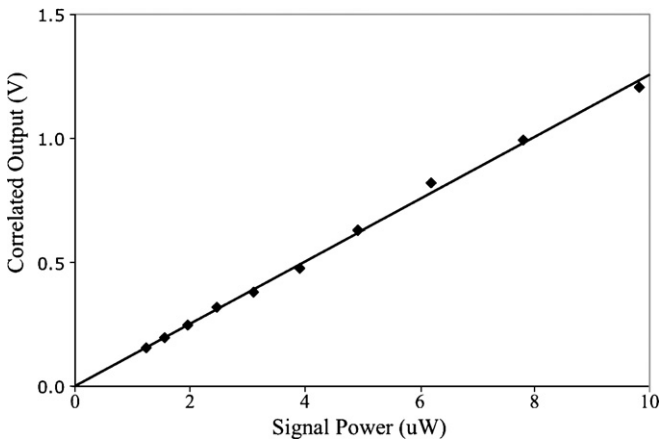

Figure 6. AMiBA correlator linearity test. While driven by large, uncorrelated noise at 1 mW, the correlator outputs linearly with its input correlated signals. The line represents the best linear fit through the data points.

degrades from its nominal value with balanced power inputs; however, the reduction in S/N remains at an acceptable level of 10%–15%.

By observing Jupiter, we have verified that better S/N could be achieved with high input power level into the correlators. The IF power imbalances are carefully controlled with the power alignment in each receiver channel, with the active temperature stabilization in the electronics, and with the adjustment of the variable gain amplifiers in the IF signal paths. The power imbalances in our system are controlled to be within 1.5 dB during a typical observation. Thus, practically, we have set the input power levels to the correlators at a nominally 0.5 mW, or −3 dBm.

Because of the wide bandwidth and nonmonotonic responses of microwave components, it is necessary to calibrate the passband properties for each baseline. This information is also essential for lag-to-visibility transformation. The correlator passband is recovered by spatially sweeping a broadband noise source across a pair of the receivers. The cross-correlation output is measured against the relative time delay between the receivers, and is Fourier-transformed to yield the spectral response of the passband. Dominated by the broadband matching circuit, the spectral structure typically shows a major gain dip in 6–12 GHz. At some extreme frequencies, the gains are off the peak value by more than 10 dB. The large fluctuations in the correlator passbands result in a narrower effective bandwidth. Further details in this part of work will be addressed in Lin et al. (2009). A correlator module with a flat spectral response across the IF band would yield a wider effective bandwidth, and thus increase the AMiBA instrument sensitivity. Alternatively, increasing the number of the lags would have had a similar benefit to our system.

4. CONCLUSION

In pursuing high sensitivity and low systematics, we have built a radio interferometer to observe the CMB and the SZE at 3 mm wavelength. The number of elements and the instantaneous bandwidth are the two critical parameters influencing the system performance of AMiBA. The sensitivity of the interferometer is roughly proportional to the number of array elements. The MMIC technology addresses component miniaturization, production capability, performance uniformity, and the state-of-the-art sensitivity. Its rapid progress in millimeter wavelength has already provided realistic ways to build compact receivers with mass production capacity, such as in the Q/U Imaging Experiment (QUIET; Samtleben 2008). The advantage of MMIC would benefit especially large-scale projects, such as the ALMA Band-1 and Band-2, as well as the Square Kilometer Array.

Large instantaneous bandwidth increases the sensitivity with its square root of the increment. For continuum sensitivity, the lag-correlator has the advantage, among other correlation techniques, to achieve very wide bandwidth operation. The major challenge is in the availability of broadband devices and circuitries to handle multioctave signals.

At millimeter wavelengths, heterodyne detection with a broad correlation bandwidth as in AMiBA would be competitive with bolometric techniques in terms of system noise and sensitivity. In addition to cosmology, broadband lag-correlators, with only coarse to moderate spectral resolution, may be suitable for redshift surveys of extragalactic objects at submillimeter wavelengths, or in the tera-hertz regime. By increasing the number of lags, it may also be practical for Galactic observations.

This is an overview of the detection system for the seven-element AMiBA array. The system has been under routine operation during the past two years at the site in the Mauna Loa Observatory, Hawaii. We are in the process to expand this array to 13 elements with 1.2 m reflectors.

We thank the Ministry of Education, the National Science Council, and the Academia Sinica for their support of this project. We thank the Smithsonian Astrophysical Observatory for hosting the AMiBA project staff at the SMA Hilo Base Facility. We thank the NOAA for locating the AMiBA project at their site on Mauna Loa. We thank the Hawaiian people for allowing astronomers to work on their mountains in order to study the universe.

REFERENCES

Bennett, C., et al. 2003, ApJS, 148, 1
Carlstrom, J. E., Holder, G. P., & Reese, E. D. 2002, ARA&A, 40, 643
Chen, M. T., et al. 2002, Proc. SPIE, 4855, 312
Clarricoats, P. J. B., & Olver, A. D. 1984, Corrugated Horns for Microwave Antennas (London: Peregrinus)
Claude, S., et al. 2005, Proc. IRMMW-THz, 2, 407
Ediss, G. A., Kerr, A. R., & Koller, D. 2000, ALMA Memo 295 (Charlottesville, VA: NRAO)
Erickson, N. R., et al. 1999, IEEE Trans. Microw. Theory Tech., 47, 2212
Goldsmith, P. 1998, Quasioptical Systems: Gaussian Beam Quasioptical Propagation and Applications (New York: Wiley)

Halverson, N. W., et al. 2002, ApJ, 568, 38
Harris, A. I., & Zmuidzinas, J. 2001, Rev. Sci. Instrum., 72, 1531
Ho, P. T. P., Moran, J. M., & Lo, K. Y. 2004, ApJ, 616, L1
Ho, P. T. P., et al. 2009, ApJ, 694, 1610
Hwang, Y.-J., et al. 2002a, IEEE Microw. Wirel. Compon. Lett., 12, 209
Hwang, Y.-J., et al. 2002b, Proc. 32nd European Microwave Conf. 1, 87
Koch, P., et al. 2009, ApJ, 694, 1670
Li, C. T., et al. 2004, Proc. SPIE, 5498, 455
Lin, K.-Y., et al. 2009, ApJ, 694, 1629
Liu, A.-S., Wu, R.-B., & Yu, Y.-C. 2003, IEEE AP-S Int. Symp. Digest, 2, 60
Lo, K. Y., et al. 2001, in AIP Conf. Proc. 586, Relativistic Astrophysics: 20th Texas Symposium, ed. J. Craig Wheeler & H. Martel (New York: AIP), 172
Nishioka, H., et al. 2009, ApJ, 694, 1637
Padin, S. 1994, IEEE Trans. Microw. Theory Tech., 43, 782
Padin, S., et al. 2002, PASP, 114, 83
Pospieszalski, M. W., et al. 2000, IEEE MTT-S Int. Symp. Digest, 1, 11
Ruze, J. 1966, Proc. IEEE, 54, 633
Samtleben, D. 2008, Proc. 43rd "Rencontres de Moriond" on Cosmology (arXiv:astro-ph/0806.4334v1)
Sunyaev, R. A., & Zel'dovich, Y. B. 1970, Comments Astrophys. Space Phys., 2, 66
Sunyaev, R. A., & Zel'dovich, Y. B. 1972, Comments Astrophys. Space Phys., 4, 173
Thompson, A. R., & D'Addario, L. R. 1982, Radio Sci., 17, 357
Umetsu, K., et al. 2009, ApJ, 694, 1643
Weinreb, S., et al. 1999, IEEE MTT-S Int. Symp. Digest, 1, 101
Wollack, E. J., Grammer, W., & Kingsley, J. 2002, ALMA Memo 425, (Charlottesville, VA: NRAO)
Wu, J.-H. P., et al. 2009, ApJ, 694, 1619
Zhang, X. 1993, IEEE Trans. Microw. Theory Tech., 41, 1263